

# Significant Glass-Transition-Temperature Increase through Hydrogen-Bonded Copolymers

SHIAO-WEI KUO,<sup>1</sup> HONGYAO XU,<sup>1,2</sup> CHIH-FENG HUANG,<sup>1</sup> FENG-CHIH CHANG<sup>1</sup>

<sup>1</sup>Institute of Applied Chemistry, National Chiao-Tung University, Hsin Chu, Taiwan

<sup>2</sup>Department of Chemistry, Anhui University, Anhui, 230039, China

Received 18 April 2002; revised 1 July 2002; accepted 16 July 2002

**ABSTRACT:** The role of hydrogen bonding in promoting intermolecular cohesion and higher glass-transition temperatures of polymer is a subject of longstanding interest. A series of poly(vinylphenol-co-vinylpyrrolidone) copolymers were prepared by the free-radical copolymerization of acetoxystyrene and vinylpyrrolidone; this was followed by the selective removal of the acetyl protective group, with corresponding and significant glass-transition-temperature increases after this procedure. The incorporation of acetoxystyrene into poly(vinylpyrrolidone) resulted in lower glass-transition temperatures because of the reduced dipole interactions in its homopolymers. However, the deacetylation of acetoxystyrene to transform the poly(vinylphenol-co-vinylpyrrolidone) copolymer enhanced the higher glass-transition temperature because of the strong hydrogen bonding in the copolymer chain. The thermal properties and hydrogen bonding of these two copolymers were investigated with differential scanning calorimetry and Fourier transform infrared spectroscopy, and good correlations between the thermal behaviors and IR results were observed. © 2002 Wiley Periodicals, Inc. *J Polym Sci Part B: Polym Phys* 40: 2313–2323, 2002

**Keywords:** glass transition; hydrogen bonding; copolymerization; association

## INTRODUCTION

A polymer possessing a higher glass-transition temperature ( $T_g$ ) is attractive in polymer science because of the strong economic incentives arising from its potential applications. For example, the  $T_g$  value of poly(methyl methacrylate) is relatively low at about 100 °C, which limits its applications in the optical electronic industry, including compact discs, optical glass,

and optical fibers. For the purpose of raising  $T_g$ , the incorporation of monomers with rigid or bulky structures to copolymerize with methyl methacrylate has been widely reported to overcome the miscibility problem through simple blending. However, the achieved  $T_g$  usually obeys or is lower than the Fox rule because of poor specific interactions between the polymer segments. From a thermodynamic viewpoint,  $T_g$  is considered a second-order thermodynamic transition that can be detected in properties such as the heat capacity and specific volume. One of the most common approaches to analyzing polymer glass transitions is the concept of free volume. In general,  $T_g$  depends on the phys-

Correspondence to: F.-C. Chang (E-mail: changfc@cc.nctu.edu.tw)

*Journal of Polymer Science: Part B: Polymer Physics*, Vol. 40, 2313–2323 (2002)  
© 2002 Wiley Periodicals, Inc.

ical and chemical nature of the polymer molecules, such as the molar mass, branching, crosslinking, and specific interactions. Over the years, various equations have been offered to predict the variation of  $T_g$ 's of random copolymers or miscible blends as a function of composition, which can be well interpreted in terms of the specific interaction within a copolymer or miscible blend.<sup>1-3</sup>

In a previous study,<sup>4</sup> we found that  $T_g$ 's of poly(vinylphenol) (PVPh)/poly(vinylpyrrolidone) (PVP) blends are significantly higher than the values predicted by the Fox rule,<sup>1</sup> indicating that this blend system must involve strong specific interactions. Furthermore, Coleman et al.<sup>5</sup> reported that a copolymer has a higher  $T_g$  than its corresponding polymer blend because of higher composition heterogeneities in the hydrogen-bonded copolymer. According to the Painter-Coleman association model,<sup>6</sup> the interassociation equilibrium constant of poly(vinylphenol-*co*-ethyl methacrylate) ( $K_A = 67.4$ ) is higher than the interassociation equilibrium constant of the PVPh/poly(ethyl methacrylate) blend ( $K_A = 37.4$ ), implying that the experimental  $T_g$  for a copolymer and blend of the same composition should be different.<sup>5</sup> This result can be reasonably explained by differences in the degree of rotational freedom due to an intramolecular screening and spacing effect.<sup>7</sup> This phenomenon can also be interpreted in terms of the correlation hole effect described by De Gennes.<sup>8</sup> Recently, Hu et al.<sup>9</sup> found that the interassociation equilibrium of a PVPh/PVP blend (from a model compound) is 6000, that is, significantly higher than  $K_2 = 21.00$  from hydroxyl dimer formation and  $K_B = 66.80$  from hydroxyl multimer formation of pure PVPh. This result implies that the tendency toward forming hydrogen bonding between PVPh and PVP dominates over the self-association forming intra-hydrogen bonding of pure PVPh.

In this study, a series of copolymers containing various vinylphenols and vinylpyrrolidones were synthesized for the comparison of their  $T_g$ 's with those of corresponding PVPh/PVP blends. However, it is well known that PVPh is difficult to synthesize directly from the vinylphenol monomer because of chain-transfer and other side reactions involved.<sup>10</sup> In general, PVPh is prepared with the protection of the phenolic hydroxyl group and is then transformed into the PVPh polymer after deprotection. Acetoxystyrene has been widely used in the preparation of PVPh and vinylphenol-

containing copolymers.<sup>11-13</sup> In this study, the poly(vinylphenol-*co*-vinylpyrrolidone) (PVPh-*co*-PVP) copolymers were prepared by the free-radical copolymerization of acetoxystyrene and vinylpyrrolidone, followed by the selective removal of the acetyl protective group. The reactivity ratio of these two monomers was determined by the method of Kelen and Tudos.<sup>14,15</sup>

## EXPERIMENTAL

### Materials

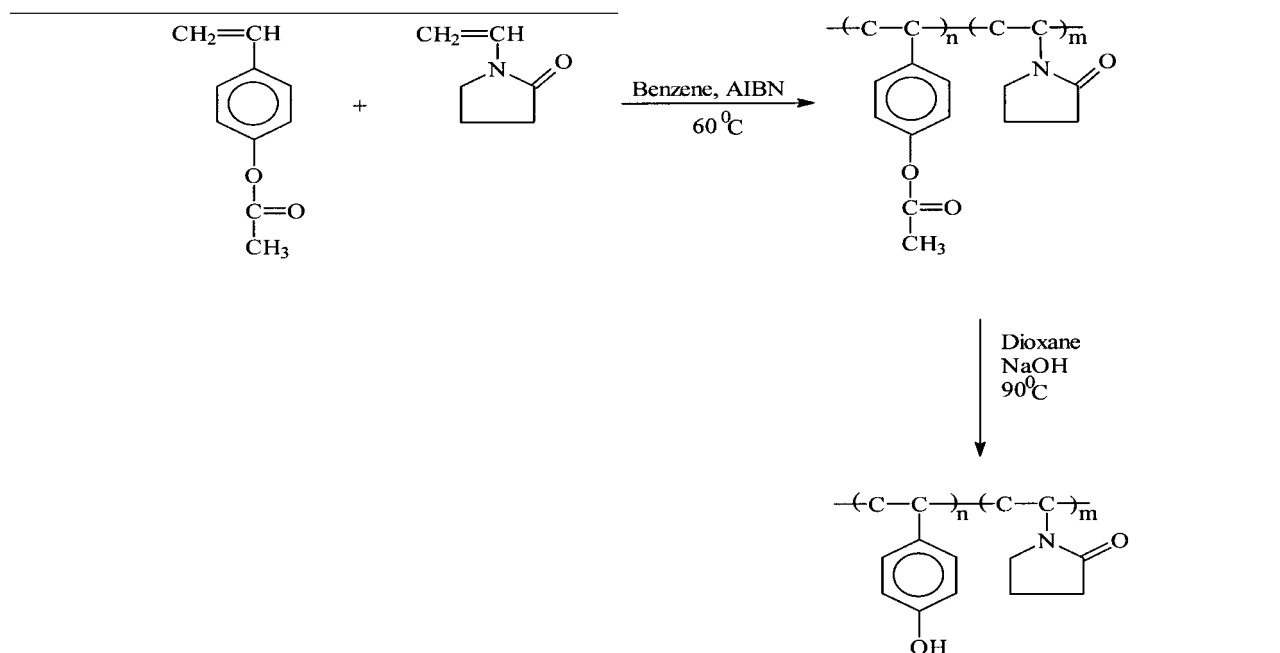
Tetrahydrofuran, benzene, cyclohexane, dioxane, vinylpyrrolidone, acetoxystyrene, and azobisisobutyronitrile (AIBN) were purchased from Aldrich Chemical Co., Inc.

### Preparation of Poly(acetoxystyrene-*co*-vinylpyrrolidone) (PAS-*co*-PVP) Copolymers

The PAS-*co*-PVP copolymers were synthesized through the free-radical copolymerization of *p*-acetoxystyrene and vinylpyrrolidone monomers in benzene with AIBN as an initiator (1 wt % based on the monomer) at 60 °C under a nitrogen atmosphere for 24 h. The product was then poured into excess cyclohexane under vigorous agitation to precipitate the copolymer. These copolymers were characterized with Fourier transform infrared (FTIR) spectroscopy, differential scanning calorimetry (DSC), and gel permeation chromatography.

### Preparation of PVPh-*co*-PVP Copolymers

PAS-*co*-PVP was dispersed in a mixture of aqueous 1 N sodium hydroxide/dioxane (10/100 w/w) and stirred for 6 h at 90 °C under a nitrogen atmosphere. The product was then poured into an excess of a hydrochloric acid solution (1 wt % aqueous solution) under vigorous agitation to precipitate the PVPh-*co*-PVP copolymer; it was then filtered and rinsed with water. The chemistry and structures can be summarized as follows:



## Characterization

### DSC

The thermal analysis was performed with a differential scanning calorimeter from DuPont (DSC-9000). The scan rate was 20 °C/min within a temperature range of 30–220 °C. The sample was quickly cooled to 0 °C from the melt for the first scan and then scanned between 0 and 300 °C at 20 °C/min.  $T_g$  is at the midpoint of the specific heat increment.

### IR Spectroscopy

IR spectra of the polymer blend films were determined with the conventional NaCl disk method at room temperature. The film used in this study was sufficiently thin to obey the Beer–Lambert law. FTIR measurements were recorded on a Nicolet Avatar 320 FTIR spectrophotometer, and 32 scans were collected with a spectral resolution of 1  $\text{cm}^{-1}$ . For the solution sample, an adequately sealed cell with NaCl windows and a 0.05-mm sample thickness was used. All model compound solutions in the absorption range obeyed the Beer–Lambert law.

## RESULTS AND DISCUSSION

### PAS-co-PVP Copolymer Analyses

Figure 1 shows scale-expanded IR spectra recorded in the region from 1620 to 1820  $\text{cm}^{-1}$  for

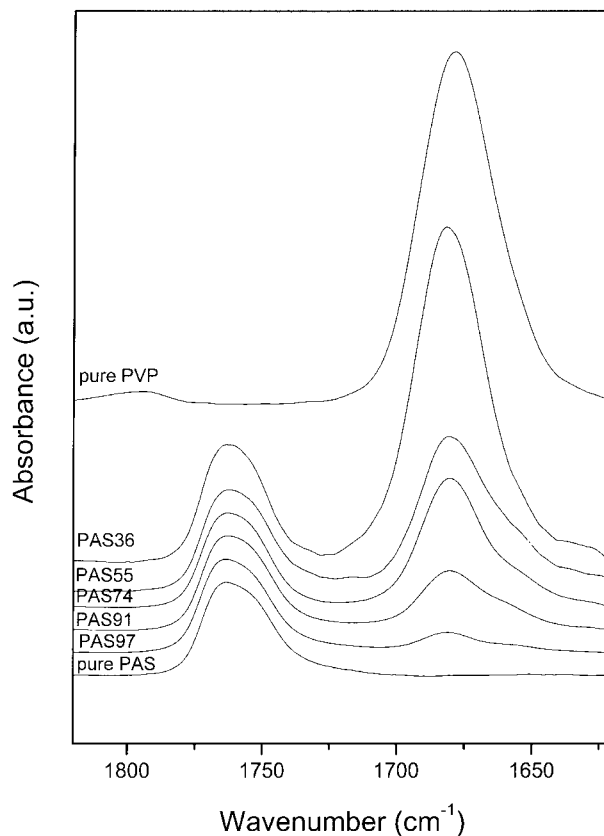


**Figure 1.** IR spectra at 1620–1820  $\text{cm}^{-1}$  for pure PS, pure PVP, and various PAS-co-PVP copolymers with different PAS contents at room temperature.

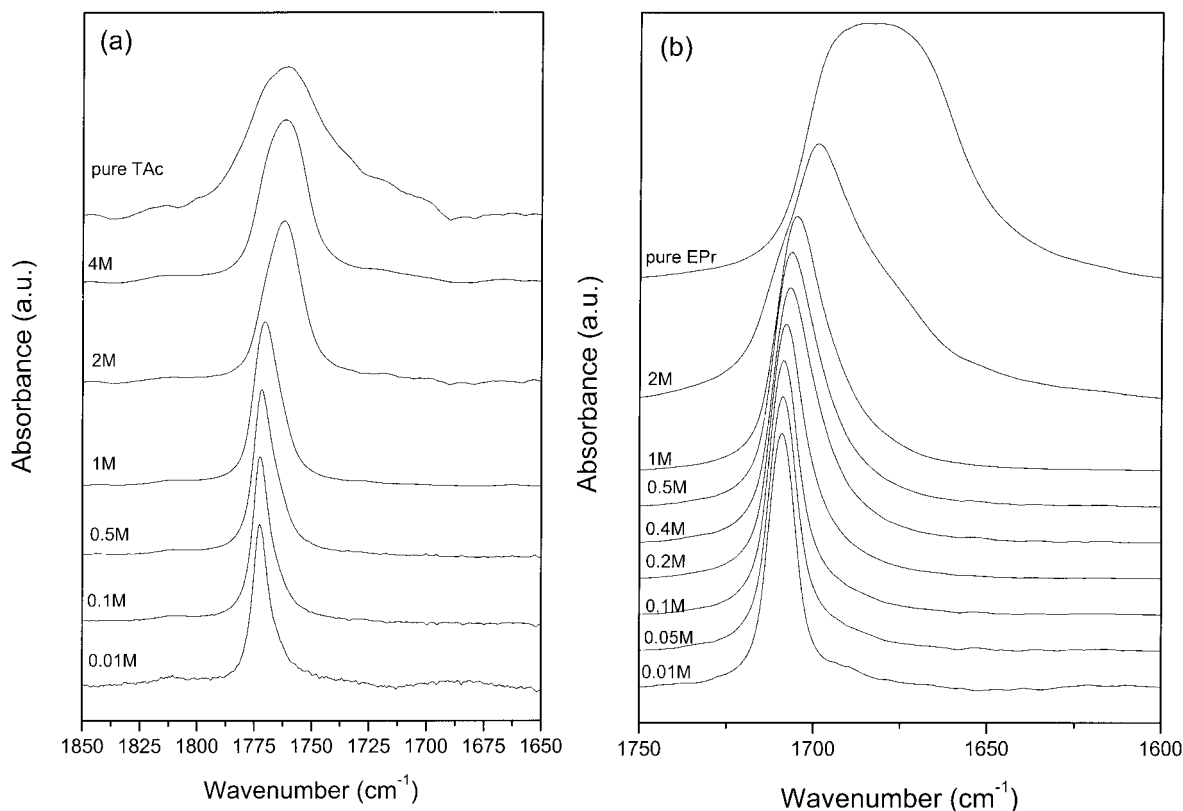


**Figure 2.** IR spectra of the carbonyl band for (a) TAc/cyclohexane and (b) EPr/cyclohexane solutions with different concentrations at room temperature.

neat poly(acetoxystyrene) (PAS), neat PVP, and various PAS-*co*-PVP copolymers at room temperature. The absorptions at 1760 and 1680  $\text{cm}^{-1}$  are assigned to the carbonyls of PAS and PVP, respectively. These bands can be decomposed into two Gaussian peaks, with areas corresponding to the PAS carbonyl (1760  $\text{cm}^{-1}$ ) and PVP carbonyl (1680  $\text{cm}^{-1}$ ). If the respective absorptivity coefficients are known, the relative molar fractions of PAS and PVP carbonyl groups can be calculated with the Beer-Lambert law. In this work, the absolute absorptivities were determined from the model compounds of *p*-tolyl acetate (TAc) and ethylpyrrolidone (EPr) for PAS and PVP, respectively. Figure 2 shows a series of different concentrations of TAc and EPr in cyclohexane, and the corresponding fitting area versus the concentrations of TAc and EPr is illustrated in Figure 3. Absolute absorptivities of 1140 and 2190 for the carbonyl bands of TAc and EPr were calculated from their slopes. To confirm these absolute absorptivities, we prepared a series of PAS/PVP

blends with known quantities of PVP and PAS to plot a calibration curve, and a good correlation was found between these two methods.<sup>16</sup> Table 1 summarizes the corresponding wave number, half-width, and curve-fitting area at the carbonyl band and the molar fraction for pure PAS, pure PVP, and various PAS-*co*-PVP copolymers. Figure 2 also reveals that the half-width toward a low frequency of the carbonyl band increased with the increase in the TAc and EPr concentrations, and this is an indication of a higher probability to form TAc/TAc and EPr/EPr self-interactions.<sup>9</sup> These results imply that certain forms of self-association exist within TAc or EPr molecules. This self-association comes from the dipole-dipole interaction, which is a function of the strength and concentration of the dipoles. Therefore, the polar group density is reduced by the incorporation of an inert diluent (nonpolar group), such as copolymerization with styrene to produce poly(styrene-*co*-acetoxystyrene)<sup>17</sup> or with ethylene to produce the ethylene-vinylacetate copolymer.<sup>18</sup>

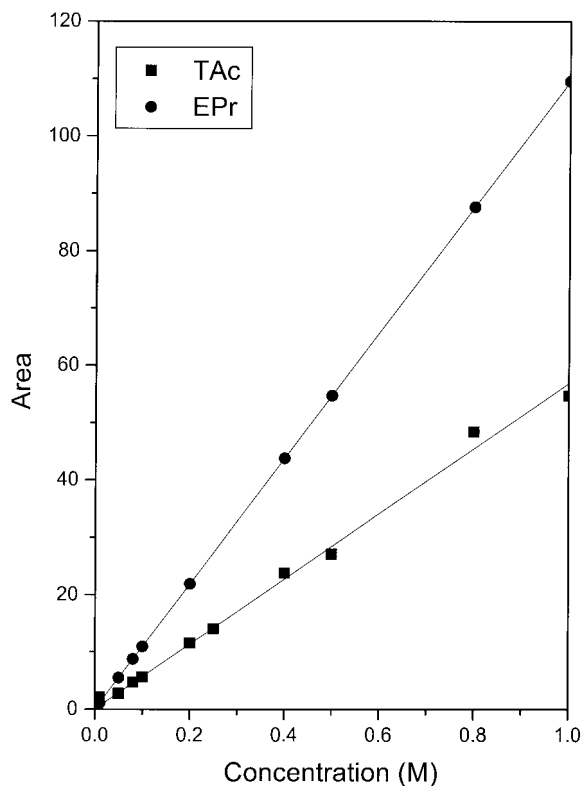


**Figure 3.** Fitting area versus the different concentrations of the model compound for (■) TAc and (●) EPr.

Figure 4 shows DSC curves of PAS-co-PVP copolymers from 60 to 180 °C, in which the single  $T_g$  is lower than the  $T_g$ 's of both mother polymers. This result is caused by the introduction of another group to reduce its self-association dipole interaction. According to Table 1, the half-width of the copolymers at 1760 and 1680  $\text{cm}^{-1}$  is sig-

nificantly decreased with an increasing molar fraction of another polymer from both individual homopolymers. In addition, both the  $T_g$  and molecular weight of the PAS-co-PVP copolymers are lower than those of both homopolymers, as has been discussed.<sup>19</sup> Therefore, the resultant  $T_g$  decrease is mainly due to a reduction in the dipole-dipole self-interaction of PAS and PVP molecules and the low molecular weight. The  $T_g$ 's and molecular weights of these synthesized PAS-co-PVP copolymers are summarized in Table 2. Table 2 also compares the monomer feed ratio and resultant copolymer composition, from which reactivity ratios were calculated with the methodology of Kelen and Tudos,<sup>14,15</sup> which was described in our previous study for the determination of the reactivity ratio.<sup>17</sup> The results are displayed graphically for PAS-co-PVP copolymers in Figure 5, from which values of  $r_{\text{PAS}} = 12.40$  and  $r_{\text{PVP}} = 0.43$  are calculated, showing a tendency toward a block copolymer.

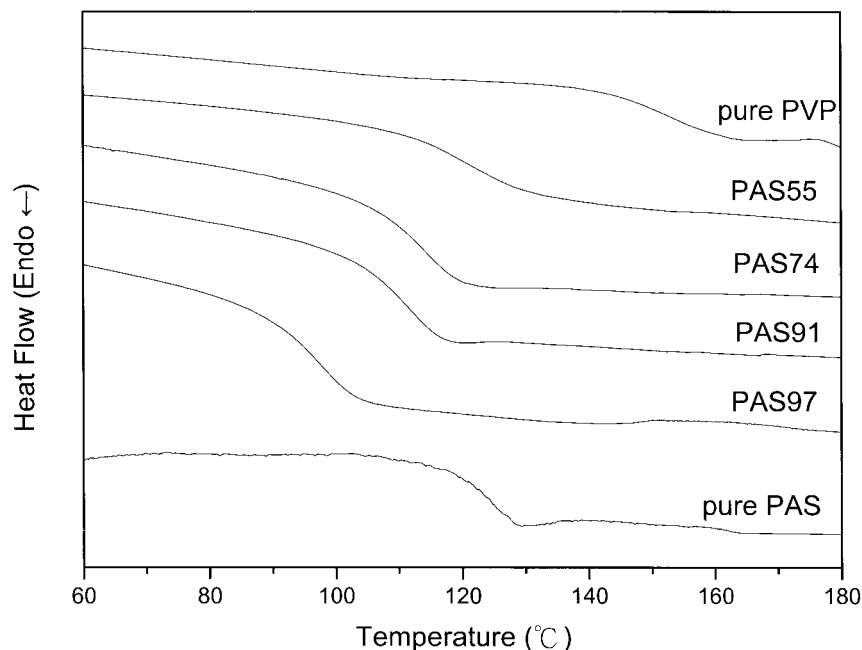
#### PVPh-co-PVP Copolymer Analyses

Figure 6 shows IR spectra recorded at room temperature in the region from 600 to 4000  $\text{cm}^{-1}$  for the PAS-co-PVP copolymer containing 9 mol % vinylpyrrolidone before and after deacetylation. The carbonyl group absorption at 1760  $\text{cm}^{-1}$  [Fig. 7(A)] totally disappears after deacetylation, whereas a broad absorbance from the hydroxyl group of PVPh-co-PVP between 3100 and 3700  $\text{cm}^{-1}$  appears. We assume that the backbone structure and vinylphenol content in the prepared PVPh-co-PVP copolymer are identical to those of the original PAS-co-PVP. Figure 7 pre-

**Table 1.** Curve-Fitting Results of the PAS-co-PVP Copolymer at Room Temperature<sup>a</sup>

Aberration	C=O for PVP			C=O for PAS			PAS (mol %)
	$\nu$ ( $\text{cm}^{-1}$ )	$W_{1/2}$ ( $\text{cm}^{-1}$ )	A (%)	$\nu$ ( $\text{cm}^{-1}$ )	$W_{1/2}$ ( $\text{cm}^{-1}$ )	A (%)	
PVP	1678.0	26.18	100	—	—	0	0
PAS6	1680.3	24.24	95.15	1760.2	19.86	4.85	5.7
PAS36	1680.9	23.95	84.81	1760.3	20.21	15.19	35.6
PAS55	1681.5	20.26	59.40	1760.3	21.20	40.60	54.7
PAS74	1682.0	20.22	38.59	1759.7	22.32	61.41	73.7
PAS91	1682.2	19.23	22.33	1760.0	23.16	77.67	91.4
PAS97	1682.4	16.63	3.04	1760.6	23.33	86.96	97.4
PAS	—	—	0	1759.3	23.67	100	100

<sup>a</sup>  $\nu$  = wavenumber;  $W_{1/2}$  = half-width; A = curve-fitting area.



**Figure 4.** DSC thermograms of pure PAS, pure PVP, and PAS-*co*-PVP copolymers with different PAS contents.

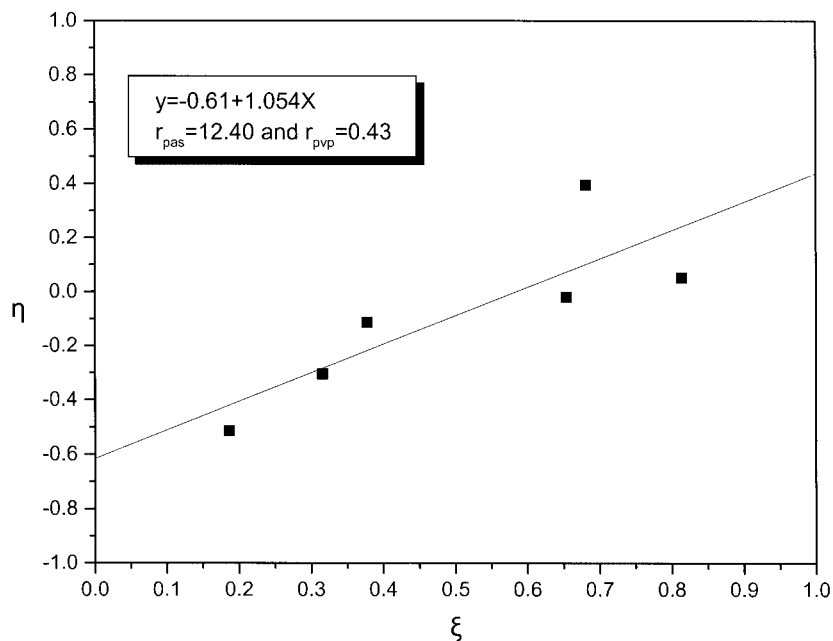
sents FTIR spectra of the carbonyl stretching recorded at room temperature and ranging from 1620 to 1710  $\text{cm}^{-1}$  for the pure PVP and various compositions of PVPh-*co*-PVP copolymers. The carbonyl stretching frequency splits into two bands at 1680 and 1651  $\text{cm}^{-1}$ , corresponding to the free and hydrogen-bonded carbonyl groups. The fraction of hydrogen-bonded carbonyl groups increases with the increase in the PVPh molar fraction in the PVPh-*co*-PVP copolymer.

Figure 8 shows DSC curves of the pure PVPh, pure PVP, and various PVPh-*co*-PVP copolymers from 90 to 230 °C. Essentially, all PVPh-*co*-PVP copolymers have only a single  $T_g$ , which is substantially higher than the  $T_g$ 's of both mother polymers. This large and positive  $T_g$  deviation indicates that a strong interaction exists between the two polymers. Figure 9 illustrates scale-expanded IR spectra in the range 2700–4000  $\text{cm}^{-1}$  for pure PVPh and various PVPh-*co*-PVP copoly-

**Table 2.** Information on PAS-*co*-PVP<sup>a</sup>

Aberration	Monomer Feed (mol %)		Polymer Composition (mol %)		$T_g$	$M_n$	Yield (%)
	PVP	AS	PVP	AS			
PVP	100	0	100	0	154.5	52,000	82
PAS6	96.4	3.6	94.3	5.7	142.1	6,000	36
PAS36	92.7	7.3	64.4	35.6	135.5	5,000	38
PAS55	84.9	15.1	45.3	54.7	122.4	4,800	43
PAS74	67.8	32.2	26.7	73.7	114.4	5,200	40
PAS91	48.4	51.6	8.6	91.4	111.7	6,100	38
PAS97	26.1	73.9	2.6	97.4	97.0	8,000	36
PAS	0	100	0	100	122.2	21,500	53

<sup>a</sup> AS = acetoxystyrene;  $M_n$  = number-average molecular weight.



**Figure 5.** Kelen-Tudos plot for PAS-co-PVP copolymers.

mers measured at room temperature. The pure PVPh has a broad band centered at  $3350\text{ cm}^{-1}$  and a shoulder at  $3525\text{ cm}^{-1}$  corresponding to the multimer hydrogen-bonded hydroxyl group and

the free hydroxyl group, respectively. The peak frequency of this broad band tends to shift toward a lower wave number with increasing PVP content. Meanwhile, the intensity of the free hy-

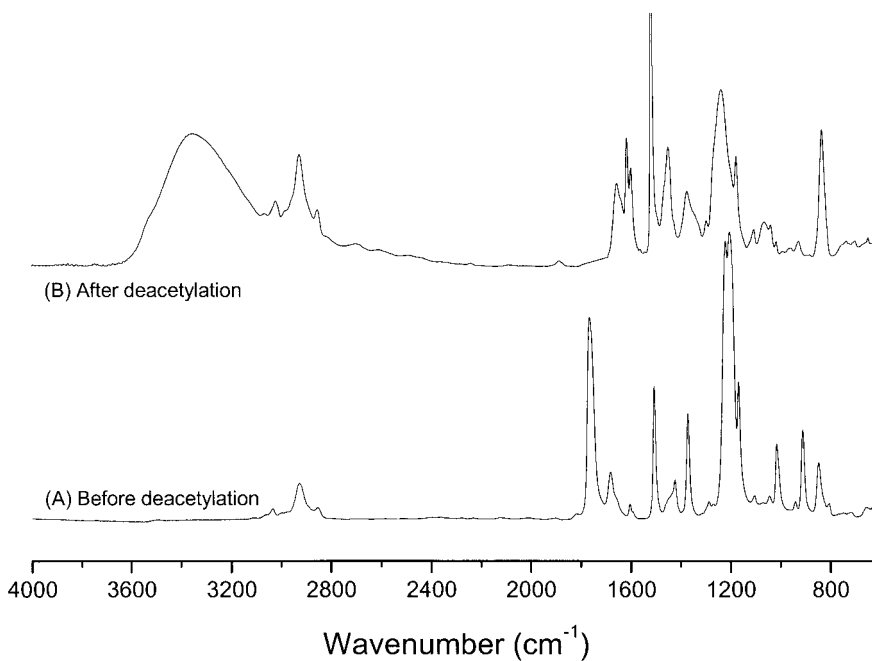


**Figure 6.** Comparison of FTIR spectra (A) before and (B) after the deacetylation reaction.



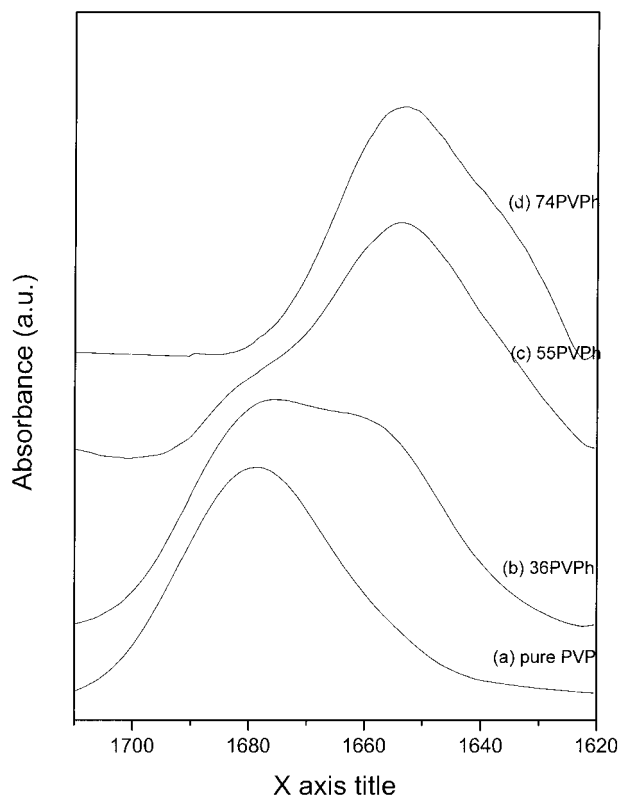


**Figure 7.** FTIR spectra recorded at room temperature in the 1620–1710-cm<sup>-1</sup> region for PVPPh-co-PVP copolymers with different PVPPh contents: (a) pure PVP, (b) 36PVPPh, (c) 55PVPPh, and (d) 74PVPPh.

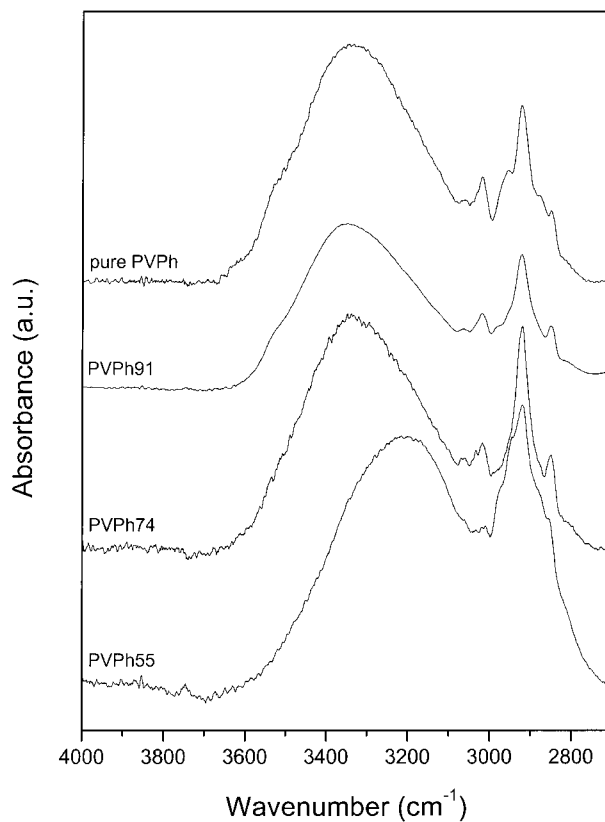


**Figure 9.** FTIR spectra recorded at room temperature in the 2700–4000-cm<sup>-1</sup> region for pure PVPPh and various PVPPh-co-PVP copolymers with different PVPPh contents.

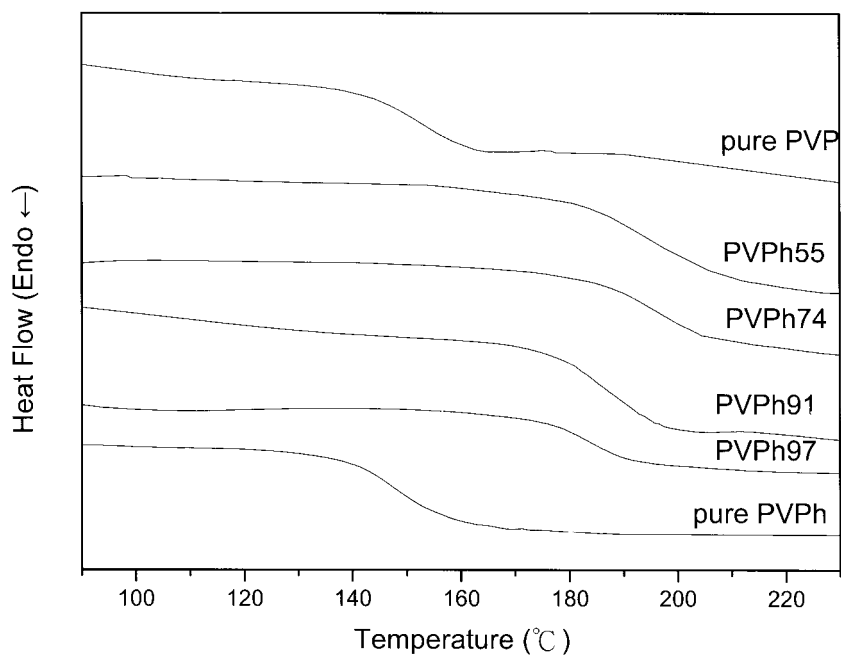


**Figure 8.** DSC thermograms of pure PVPPh, pure PVP, and PVPPh-co-PVP copolymers with different PVPPh contents.



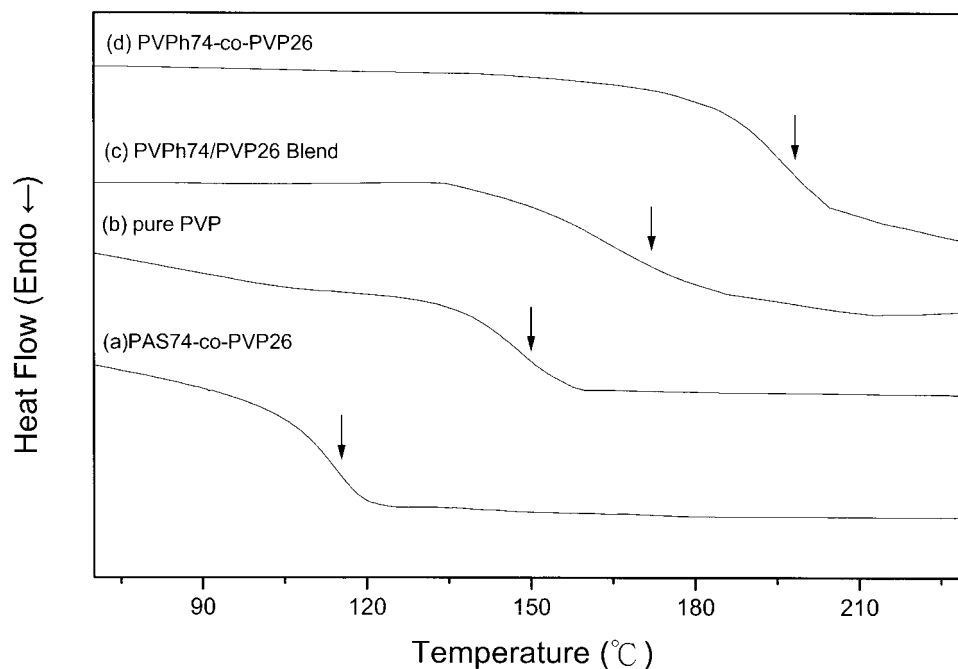


**Figure 10.** DSC thermograms of PAS74-*co*-PVP26, pure PVP, PVPh74/PVP26, and PVPh74-*co*-PVP26 (26 mol % PVP).

droxyl group decreases gradually with the increase in the PVP content, reflecting the redistribution of hydrogen bonds between hydroxyl–hydroxyl and hydroxyl–carbonyl specific interactions. The average strength of the intermolecular interaction can be roughly estimated by the extent of the frequency difference ( $\Delta\nu$ ) between the hydrogen-bonded hydroxyl absorption and free hydroxyl absorption.<sup>20</sup>  $\Delta\nu = 325 \text{ cm}^{-1}$  for 55/45 PVPh-*co*-PVP is obtained, which is significantly greater than that of the self-association between hydroxyl and hydroxyl of the pure PVPh polymer ( $\Delta\nu = 175 \text{ cm}^{-1}$ ); this result is consistent with the observed larger and positive deviation of  $T_g$ .

### Significant $T_g$ Increase Analyses

Figure 10 shows DSC analyses of the PAS74-*co*-PVP26 copolymer, pure PVP homopolymer, PVPh74/PVP26 blend, and PVPh74-*co*-PVP26 copolymer from 90 to 230 °C. The observed  $T_g$ 's are in the following order: PVPh-*co*-PVP copolymer (195 °C) > PVPh/PVP blend (175 °C) > pure PVP polymer (150 °C) > PAS-*co*-PVP copolymer (115 °C). The significant  $T_g$  increase is very interesting for us as we investigate which specific interaction exists in these polymer systems at the same mo-

lar fraction of PVP. Figure 10 also indicates that the glass-transition width of the PVPh-*co*-PVP copolymer is narrower than that of the corresponding PVPh/PVP blend with an identical molar fraction, implying that the copolymer is more homogeneous on a molecular scale than the blend system.

Figure 11 shows FTIR spectra of the carbonyl stretching recorded at room temperature from 1620 to 1730  $\text{cm}^{-1}$  with various EPr concentrations in the cyclohexane (EPr, a model compound for PVP), pure PVP, PAS74-*co*-PVP26, PVPh74/PVP26 blend, and PVPh74-*co*-PVP26 copolymer. The wave number and half-width significantly depend on the dipole interaction or hydrogen bonding on molecules or polymer chains. The carbonyl band becomes broader and shifts to a low wave number with increasing EPr concentration in cyclohexane because of the increasing probability of pyrrolidone/pyrrolidone interactions. The pure PVP shifts to a lower wave number and possesses a broader half-width relative to the EPr solution in cyclohexane because there is no inert diluent (nonpolar group) in the pure PVP and the probability of dipole–dipole interactions is expected to be greater, as mentioned previously. The half-width of the pure PVP at 1680  $\text{cm}^{-1}$

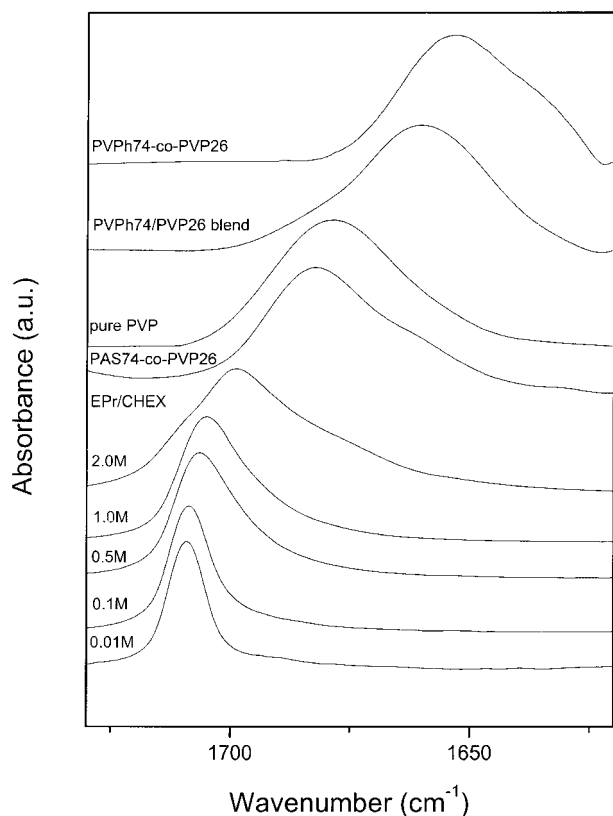


**Figure 11.** FTIR spectra recorded at room temperature in the 1620–1730- $\text{cm}^{-1}$  region for various EPr concentrations in the cyclohexane, PAS74-*co*-PVP26 copolymer, pure PVP, PVPh74/PVP26 blend, and PVPh74-*co*-PVP26 copolymer.

decreases and shifts to a higher wave number at  $1682\text{ cm}^{-1}$  with the incorporation of the acetoxy-styrene monomer into PVP chain (PAS74-*co*-PVP26). As a result,  $T_g$  of the PAS-*co*-PVP copolymer is significantly decreased with respect to the PVP because of the lower dipole interaction of the pyrrolidone moieties in the polymer chain. However, after deacetylation of PAS-*co*-PVP into PVPh-*co*-PVP, the carbonyl absorption shifts from  $1680$  to  $1651\text{ cm}^{-1}$ . This shift is attributed to the formation of hydrogen bonding between vinyl-phenol and vinylpyrrolidone segments of the copolymer. However, the same carbonyl stretching frequency of the PVPh/PVP blend shifts only to  $1660\text{ cm}^{-1}$ . This observed difference could be interpreted as follows: the number or strength of hydrogen bonds within the PVPh-*co*-PVP copolymer is greater or stronger than the corresponding PVPh/PVP blend, and this is consistent with the observed  $T_g$  difference between the PVPh-*co*-PVP

copolymer and the PVPh/PVP blend. An FTIR analysis gives the relative strength of the specific interaction in the following order: PVPh-*co*-PVP copolymer > PVPh/PVP blend > pure PVP > PAS-*co*-PVP copolymer.

Figure 12 plots  $T_g$  versus different PVP molar fractions for PAS-*co*-PVP copolymers, PVPh/PVP blends, and PVPh-*co*-PVP copolymers.  $T_g$ 's of PVPh-*co*-PVP copolymers are approximately  $90\text{ }^\circ\text{C}$  higher than those of PAS-*co*-PVP copolymers and also are about  $20\text{ }^\circ\text{C}$  greater than those of PVPh/PVP blends. The significant  $T_g$  increase between PVPh-*co*-PVP and PAS-*co*-PVP is caused by the transformation of the relatively weak dipole interaction of PAS-*co*-PVP copolymers into relatively stronger hydrogen bonding in PVPh-*co*-PVP copolymers. However, the observed higher  $T_g$ 's of PVPh-*co*-PVP copolymers in comparison with those of their corresponding PVPh/PVP blends are due to the chain connectivity, intramolecular screening, and spacing effect in the hydrogen-bonded copolymers.

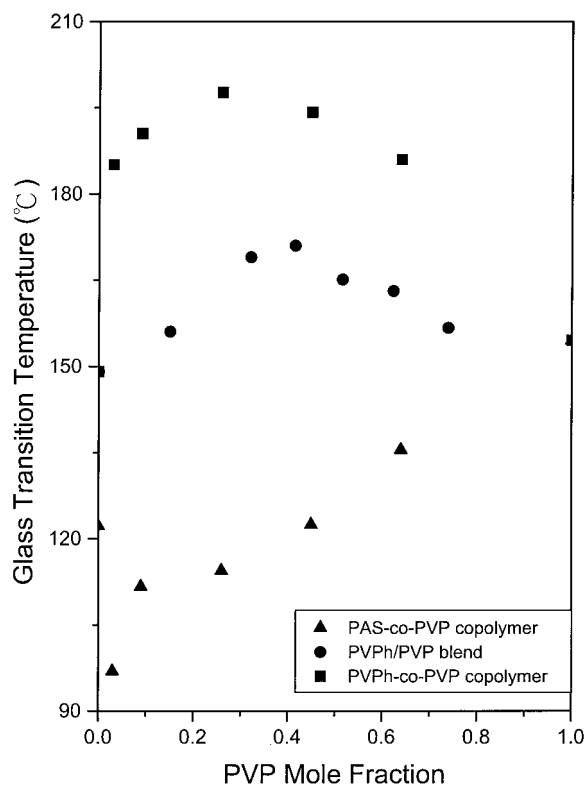


**Figure 12.** Glass-transition temperature of (▲) PAS-*co*-PVP copolymers, (●) PVPh/PVP blends, and (■) PVPh-*co*-PVP copolymers versus different PVP fractions.

In general, the  $T_g$  value of a polymer depends on the physical and chemical nature of the polymer structure, such as the molar mass, branching, and crosslinking. Hydrogen bonding gives much greater chain interaction than dipole-dipole interaction and results in higher  $T_g$ 's. Inter-chain multiple hydrogen bonding can be considered physical crosslinking. The PVPh-*co*-PVP copolymer provides a better environment for more hydrogen bonds per unit volume than the corresponding PVPh/PVP blends and results in higher  $T_g$ 's. This result provides an alternative approach to creating a higher  $T_g$  material through structural design.

## CONCLUSIONS

Copolymerizations for a series of PVPh-*co*-PVP copolymers containing various vinylphenol contents were prepared and studied. The incorporation of acetoxystyrene into PVP results in lower  $T_g$ 's because of the reduction in the dipole interaction in its respective homopolymer. However, the deacetylation of acetoxystyrene to transform the PVPh-*co*-PVP copolymer is able to enhance the higher  $T_g$  because of the strong hydrogen bonding in the copolymer chain. FTIR studies provide positive evidence of the hydrogen bonding between the hydroxyl group and carbonyl group of the PVPh-*co*-PVP copolymer and PVPh/PVP blend. FTIR also gives the relative strength of the specific interaction in the following order: PVPh-*co*-PVP copolymer > PVPh/PVP blend > pure PVP homopolymer > PAS-*co*-PVP copolymer. This is consistent with  $T_g$  behaviors.

This research was financially supported by the National Science Council (Taiwan, Republic of China) under contract NSC-90-2216-E-009-026.

## REFERENCES AND NOTES

1. Fox, T. G. *J Appl Bull Am Phys Soc* 1956, 1, 123.
2. Gordon, M.; Taylor, J. S. *J Appl Chem* 1952, 2, 493.
3. Kwei, T. *J Polym Sci Polym Lett Ed* 1984, 22, 307.
4. Kuo, S. W.; Chang, F. C. *Macromolecules* 2001, 34, 5224.
5. Coleman, M. M.; Xu, Y.; Painter, P. C. *Macromolecules* 1994, 27, 127.
6. Coleman, M. M.; Graf, J. F.; Painter, P. C. *Specific Interactions and the Miscibility of Polymer Blends*; Technomic: Lancaster, PA, 1991.
7. Painter, P. C.; Veytsman, B.; Kumar, S.; Graf, J. F.; Xu, Y.; Coleman, M. M. *Macromolecules* 1997, 30, 932.
8. De Gennes, P. G. *Scaling Concept in Polymer Physics*; Cornell University Press: Ithaca, NY, 1979.
9. Hu, Y.; Motzer, H. R.; Etxeberria A. M.; Fernandez-Berridi, M. J.; Iruin, J. J.; Painter, P. C.; Coleman, M. M. *Macromol Chem Phys* 2000, 201, 705.
10. Kato, M. *J Polym Sci Part A-1: Polym Chem* 1969, 7, 2175.
11. Kuo, S. W.; Chang, F. C. *Macromolecules* 2001, 34, 7737.
12. Zhu, K. J.; Chen, S. F.; Ho, T.; Perace, E. M.; Kwei, T. K. *Macromolecules* 1990, 23, 150.
13. Edgecombe, B. D.; Stein, J. A.; Frechet, J. M.; Xu, Z.; Kramer, E. J. *Macromolecules* 1998, 31, 1292.
14. Kennedy, J. P.; Kelen, T.; Tudos, F. F. *J Polym Sci Polym Chem Ed* 1975, 13, 2277.
15. Kelen, T.; Tudos, F. F. *Macromol Sci Chem* 1975, 9, 1.
16. Xu, H.; Kuo, S. W.; Lee, J. S.; Chang, F. C. *Polymer*, in press.
17. Kuo, S. W.; Chang, F. C. *Polymer* 2001, 43, 9843.
18. Painter, P. C.; Pehlert, G. J.; Hu, Y.; Coleman, M. M. *Macromolecules* 1999, 32, 2055.
19. O'Driscoll, K.; Sanayei, R. A. *Macromolecules* 1991, 24, 4479.
20. Moskala, E. J.; Varnell, D. F.; Coleman, M. M. *Polymer* 1985, 26, 228.